

Analysis and Modeling of HVSR in the Presence of a Velocity Inversion: The Case of Venosa, Italy

by Domenico Di Giacomo, Maria Rosaria Gallipoli, Marco Mucciarelli,
Stefano Parolai, and Sandra M. Richwalski

Abstract The aim of this work is to check the stability of the horizontal-to-vertical spectral ratios (HVSRs) calculated at the Venosa station site (Italy). This site lies over a layer of anthropogenic fill (4 m thick), a rigid layer of conglomerates (15 m thick), and a thick layer of clays (about 300 m thick) above the seismic bedrock. The velocity inversion, which takes place at the conglomerates–clays interface, is of main importance for the amplification behavior of this site. We have analyzed nearly 2 years of data, composed of 244 triggered noise records and 44 earthquakes. The results obtained by the two data sets show different site-response characteristics. In particular, the earthquake HVSR is not deamplified in the frequency range 1–8 Hz like the triggered noise HVSR. To find out the origin of this difference, we modeled both the triggered noise and the earthquakes, taking advantage of an improved version of the Thompson–Haskell propagation matrix method. The differences between triggered-noise- and earthquake-amplification functions might be explained by the difference in composition and propagation of the seismic wave fields. Moreover, we show that the nonlinear behavior of the anthropogenic fill might explain the presence of the misfit of the resonance frequency attributed to this layer between triggered noise and earthquakes.

Introduction

Surface geology has long been recognized to affect the intensity of the ground shaking. In particular, sites characterized by soft soils amplify the ground motion in specific frequency bands. Therefore, the site effect produced by the sedimentary covering has to be quantified. Recently, the horizontal-to-vertical spectral ratio (HVSR) technique (Nakamura, 1989, 2000) has been used by many authors (for a detailed review see Mucciarelli and Gallipoli, 2001) as one of the cheapest ways to study site effects by using ambient seismic noise. This technique utilizes the Fourier amplitude spectral ratio between the horizontal and the vertical component of the signal recorded at the surface at a given site to estimate the presence of site effects. Its wide use is due to the difficulty in finding a reliable reference site for application of the reference site method (RSM; Borchardt, 1970). Lermo and Chavez-Garcia (1993) proved that the HVSR technique can also be applied to the strongest part of the earthquake recordings (*S* waves). Since then, many studies (among others, Lachet and Bard, 1994; Castro *et al.*, 1997; Mucciarelli, 1998; Parolai *et al.*, 2004) have been accomplished to determine the applicability and the limitations of the HVSR technique, both for earthquakes and seismic noise. It is commonly accepted, however, that the HVSR technique permits detection of the fundamental resonance frequency

of soft deposits, even though the amplification values can be quite different from those obtained with other site-response estimation techniques (besides the RSM technique, the generalized inversion technique, coda-wave method, etc.), as explained by Field and Jacob (1995), Bonilla *et al.* (1997), Riepl *et al.* (1998), and Parolai *et al.* (2000).

In this article, we report on investigating the stability of the HVSR at the Venosa station site (southern Italy) by analyzing triggered noise and earthquake recordings. The main feature of the Venosa site is the presence of a shallow velocity inversion in the seismic-velocity profile that might be of fundamental importance for the characteristics of the HVSR of this site. The shallow velocity inversion is a common feature of many sites in Italy, and it may represent a problem for simplified zonation methods like V_s30 . We show whether the characteristics of the HVSR are influenced by:

1. the existence of any periodicity pattern in the time sequences
2. an azimuthal dependence of the fundamental frequency (for earthquakes only)
3. a dependence on the choice of the horizontal recording component (for earthquakes and triggered noise)
4. the correlation between amplitude of the recordings and fundamental frequency.

In addition, we present the conclusions drawn from comparing the HVSR of real data with those of synthetic data.

Geological Setting

The horizontally layered sedimentary cover at the Venosa station site is characterized by, from the surface down, a layer of anthropogenic fill (4 m thick), a hard layer of conglomerates (15 m thick), and a thick layer of soft clays (about 300 m thick) above the formation that we can consider as the seismic bedrock. The main characteristic of this site is a distinct *S*-wave velocity decrease at the conglomerates–clays interface; below the interface, the seismic-velocity profile regains a normal increasing trend. The presence of the velocity inversion is confirmed by Cone Penetration Test (CPT) geotechnical tests.

Data

The station at Venosa is equipped with a tridirectional seismometer Lennartz Le-3D Lite coupled with a 24-bit PRAXS-10 analog-to-digital converter. The sampling rate is 125 samples/sec and the sensor shows equal characteristics on the three components. The station works only on trigger so that the noise recordings are nonstationary and of relatively high amplitude (triggered noise). The use of the triggered noise stems from the observation that the HVSR of such signals is able to satisfactorily reproduce the HVSR response of the earthquakes (Mucciarelli *et al.*, 2003).

Among the available data, we analyzed 152 recordings from November 2001 to March 2002 (at least one recording per day), and 92 recordings from April 2002 to July 2003 of triggered noise. These were selected to have a good temporal coverage for each month of available recordings. This selection was done to verify whether the HVSR characteristics of the Venosa station site are affected by seasonal changes.

For nearly 2 years, this station has recorded several earthquakes (local, regional, and teleseismic events) covering a wide range of epicentral distances and azimuths. Table 1 lists the parameters of the local events, and Table 2 lists the parameters of the earthquakes of the San Giuliano di Puglia 2002 sequence. Because the regional and teleseismic events were analyzed in the same way, their parameters are listed jointly in Table 3. The local seismicity (Fig. 1) is mainly characterized by events ($1.9 < M_L < 5.4$) from the Apennines, the Gargano's Cape, and the San Giuliano di Puglia area. Tables 1, 2, and 3 list only earthquakes that show a signal-to-noise ratio greater than 3 in the frequency range 0.2–25 Hz (in total, 44) and whose results we will examine next.

Method and Results

To compute the spectral ratios, all time series were tapered with a 5% cosine function. We performed the fast

Fourier transform (FFT) for each component, and the amplitude spectra were smoothed by using the Konno and Ohmachi (1998) window ($b = 20$). We first computed the spectral ratios using the north–south and east–west component spectra separately. This step was carried out both for the triggered noise and the earthquake recordings to verify the presence of any directional effect on the HVSR characteristics, but because we found no significant differences, we only show the HVSRs obtained using the root-mean-square average spectrum (rms average). Moreover, the fact that the two separate components yield equal HVSR, allows us to take into account 1D propagation only in the modeling described in the following section.

For triggered noise a generally accepted rule of thumb is that the shortest window length of the seismic noise signals has to be selected in such a way as to include at least 10 cycles of the lowest frequency analyzed (Bard, 1998; Parolai *et al.*, 2001). We used windows of the maximum available length (50 sec). This window length can be considered long enough to accomplish the analysis up to the lowest frequency of interest, which is 0.2 Hz.

All analyzed earthquake recordings were detrended, baseline corrected, and bandpass filtered between 0.2 and 25 Hz to remove the frequencies normally dominated by mechanical and electronic noise. The Fourier spectra were calculated on a time window of 20 sec starting at 1 sec before the onset of the *S* waves. In contrast, we did not select a specific phase for the regional and teleseismic events (Table 3) but took the longest possible time window from the first arrival ($40 \text{ sec} < \text{window length} < 65 \text{ sec}$; see Riepl *et al.*, 1998).

HVSR-Triggered Noise

Figure 2 shows the results of the analysis of the triggered noise. Two distinct peaks are present, one at high frequency (about 14.5 Hz) and one at low frequency (0.4–0.5 Hz), as well as a clear deamplification in the frequency range 1–8 Hz. A rapid calculation using the formula $f = V_s/4h$ and considering reasonable velocities for this kind of sediment from standard literature values, allows us to correlate the high-frequency peak to the anthropogenic fill–conglomerates interface, whereas the clays–seismic bedrock interface gives rise to the low-frequency peak.

HVSR Earthquakes and Comparison with HVSR-Triggered Noise

Figure 3a–c compares, respectively, the HVSR of the triggered noise with the HVSR of the local, San Giuliano di Puglia 2002 sequence, and regional and teleseismic events. Moreover, because the characteristics of the HVSRs of the earthquakes may depend on the incidence angle (see Lermo and Chavez-Garcia, 1993; Parolai and Richwalski, 2004), we show in Figure 3d the HVSR of all the analyzed earthquakes to average out this effect. The comparison shows the

Table 1
Parameters of the Local Earthquakes

| Event | Date (dd/mm/yy) | Time, UTM* | Latitude | Longitude | M_L | Epicentral Distance (km) | Back-Azimuth (°N) |
|-------|--------------------|---------------|----------|-----------|-------|-----------------------------|----------------------|
| 1 | 20/11/01 | 18.29.34 | 41.8 | 16.1 | 3.3 | 96.8 | 9.9 |
| 2 | 30/11/01 | 03.17.29 | 41.7 | 15.8 | 3.5 | 82.5 | 354.9 |
| 3 | 09/12/01 | n.a. | 40.8 | 15.3 | 3.2 | 46.7 | 243.2 |
| 4 | 13/04/02 | 17.04.35 | 40.6 | 16.6 | 3.3 | 78.2 | 116.9 |
| 5 | 18/04/02 | 20.56.31 | 40.7 | 15.7 | 4.1 | 31.4 | 193.6 |
| 6 | 03/02/03 | 11.24.24 | 40.753 | 15.643 | 3.6 | 29.3 | 206.8 |
| 7 | 03/02/02 | 12.18.39 | 40.751 | 15.669 | 3.5 | 28.4 | 202.6 |
| 8 | 04/02/03 | 8.31.33 | 40.783 | 15.661 | 2.8 | 26.3 | 207.8 |
| 9 | 29/04/03 | 18.45.39 | 41.626 | 16.217 | 3.6 | 80.8 | 20.1 |
| 10 | 24/05/03 | 14.46.32 | 40.8 | 15.23 | 3.2 | 52.8 | 245 |
| 11 | 24/07/03 | 4.57.56 | 41.86 | 15.657 | 3.6 | 100.3 | 348 |
| 12 | 27/07/03 | 16.09.56 | 40.586 | 15.581 | 2.9 | 46.9 | 200.5 |

UTC, coordinated universal time.

Table 2
Parameters of the Earthquakes of the San Giuliano di Puglia 2002 Sequence

| Event | Date (dd/mm/yy) | Time, UTM | Latitude | Longitude | M_L | Epicentral Distance (km) | Back-Azimuth (°N) |
|-------|--------------------|--------------|----------|-----------|-------|-----------------------------|----------------------|
| 1 | 31/10/02 | 10.33.15 | 41.76 | 14.94 | 5.4 | 114.8 | 316 |
| 2 | 31/10/02 | 13.04.03 | 41.67 | 14.89 | 3.7 | 110.2 | 311 |
| 3 | 31/10/02 | 16.56.55 | n.a. | n.a. | 3.6 | n.a. | n.a. |
| 4 | 31/10/02 | 21.33.35 | 41.72 | 14.83 | 3.4 | 117.7 | 331.2 |
| 5 | 01/11/02 | 22.56.59 | 41.43 | 14.87 | 1.9 | 94.7 | 298.8 |
| 6 | 01/11/02 | 00.41.05 | 41.71 | 14.91 | 2.9 | 112.3 | 313.2 |
| 7 | 01/11/02 | 15.09.03 | 41.69 | 14.83 | 5.3 | 115.4 | 310 |
| 8 | 01/11/02 | 15.20.04 | 41.74 | 14.85 | 4.1 | 118.1 | 312.5 |
| 9 | 01/11/02 | 15.42.09 | 41.72 | 14.84 | 3.4 | 117.1 | 311.5 |
| 10 | 01/11/02 | 17.21.15 | 41.71 | 14.81 | 4.3 | 118.1 | 310.3 |
| 11 | 01/11/02 | 22.44.13 | 41.69 | 14.8 | 3.8 | 117.2 | 309.2 |
| 12 | 02/11/02 | 2.26.21 | 41.72 | 14.81 | 3.7 | 118.9 | 310.6 |
| 13 | 02/11/02 | 2.37.07 | 41.72 | 14.81 | 3.7 | 118.9 | 310.6 |
| 14 | 02/11/02 | 6.22.06 | 41.69 | 14.81 | 3.8 | 116.6 | 309.5 |
| 15 | 02/11/02 | 23.28.16 | 41.684 | 14.887 | 3.9 | 111.5 | 311.5 |
| 16 | 02/11/02 | 23.59.08 | 41.693 | 14.928 | 3.7 | 109.9 | 313.1 |
| 17 | 03/11/02 | 14.34.24 | 41.633 | 14.817 | 3.3 | 111.9 | 307.3 |
| 18 | 04/11/02 | 1.17.00 | n.a. | n.a. | n.a. | n.a. | n.a. |
| 19 | 04/11/02 | 3.26.45 | 41.741 | 14.805 | 4.1 | 120.8 | 311.3 |
| 20 | 05/11/02 | 23.10.31 | 41.714 | 14.934 | 3.7 | 111.2 | 314.1 |
| 21 | 11/11/02 | 18.32.21 | 41.664 | 14.873 | 3.5 | 110.8 | 310.2 |
| 22 | 12/11/02 | 9.27.45 | 41.677 | 14.799 | 4.2 | 116.3 | 308.6 |
| 23 | 13/11/02 | 2.52.02 | 41.715 | 14.814 | 3.4 | 118.3 | 310.6 |
| 24 | 29/04/03 | 10.47.38 | 41.611 | 14.962 | 3.6 | 101.3 | 310.8 |

Table 3
Parameters of the Regional and Teleseismic Events

| Event | Date (dd/mm/yy) | Time, UTM | Latitude | Longitude | Epicentral Distance (km) | Back-Azimuth (°N) | M_b | Epicenter Area |
|-------|--------------------|--------------|----------|-----------|-----------------------------|----------------------|---------------|----------------------|
| 1 | 22/01/02 | 4.56.06 | 35.7 | 26.7 | 1132 | 114 | 6.2 | Crete |
| 2 | 09/05/02 | 1.51.19 | 36.5 | 23.2 | 889 | 121 | 4.8 (M_L) | Southern Greece |
| 3 | 31/10/02 | 2.27.09 | 37.8 | 14.92 | 361 | 188 | 3.5 (M_L) | Sicily (Etna) |
| 4 | 02/12/02 | 4.59.53 | 38 | 21 | 558 | 120 | n.a. | Greece |
| 5 | 02/04/03 | 3.53.11 | 35.3 | -35.6 | 4754 | 275 | 6.1 | North Atlantic Ridge |
| 6 | 10/04/03 | 0.42.22 | 38.2 | 26.9 | 1014 | 99 | 5.6 | Aegean Sea |
| 7 | 17/04/03 | 22.36.41 | 38.2 | 26.8 | 1006 | 100 | 4.5 | Southern Greece |
| 8 | 29/04/03 | 1.52.51 | 38.2 | 26.8 | 1006 | 100 | 4.5 | Southern Greece |

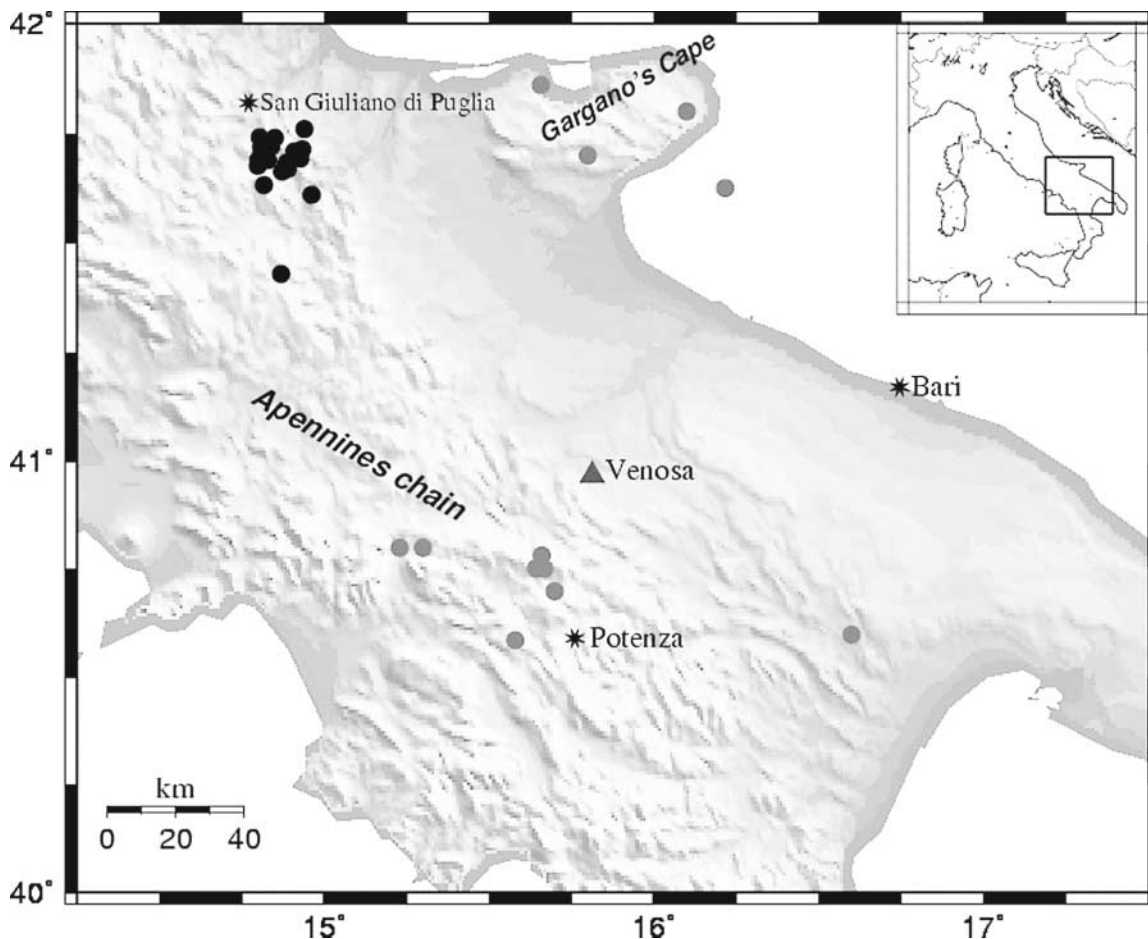


Figure 1. Map showing the location of the station of Venosa (filled triangle), the epicenters of the local earthquakes (gray circles), and the San Giuliano di Puglia 2002 sequence (black circles). Map plotted using GMT by Wessel and Smith (1991).

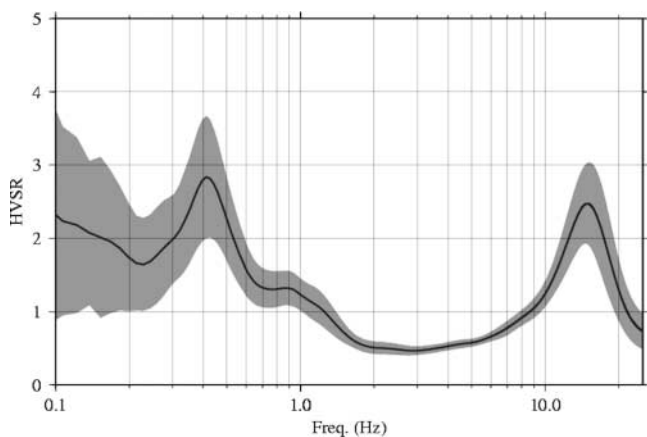


Figure 2. Mean spectral ratio of the triggered noise (black solid line) \pm 1 standard deviation (S.D.) (shaded area)

evidently different characteristics of the HVSR of the earthquakes from the HVSR of the triggered noise. In particular, the HVSR of the earthquakes does not exhibit deamplification ($HVSR < 1$) in the frequency range 1–8 Hz, even though the amplification is not very high (generally about a value 2). In addition, the high-frequency peak of the HVSR of the earthquakes occurs at about 12.5 Hz, which is about 2 Hz lower than for the triggered noise. On the contrary, the low-frequency peaks show an excellent correlation. However, the origin of the misfit of the peak at high frequency can be related neither to the effect of the azimuth of the analyzed earthquakes (no correlation observed; Fig. 4a) nor to seasonal changes (no periodicity pattern; Fig. 4b). Subsequently, we focused on the possibility that the fundamental resonance frequency of the anthropogenic fill has some dependence on the amplitude of all the analyzed signals. For this purpose, we determined the positive (PGV^+) and negative (PGV^-) peak horizontal velocities of each signal and calculated the difference ($\Delta PGV = PGV^+ - PGV^-$). Then, we constructed the semi-logarithmic diagram shown in Figure 5. It is significant that in increasing the ground motion

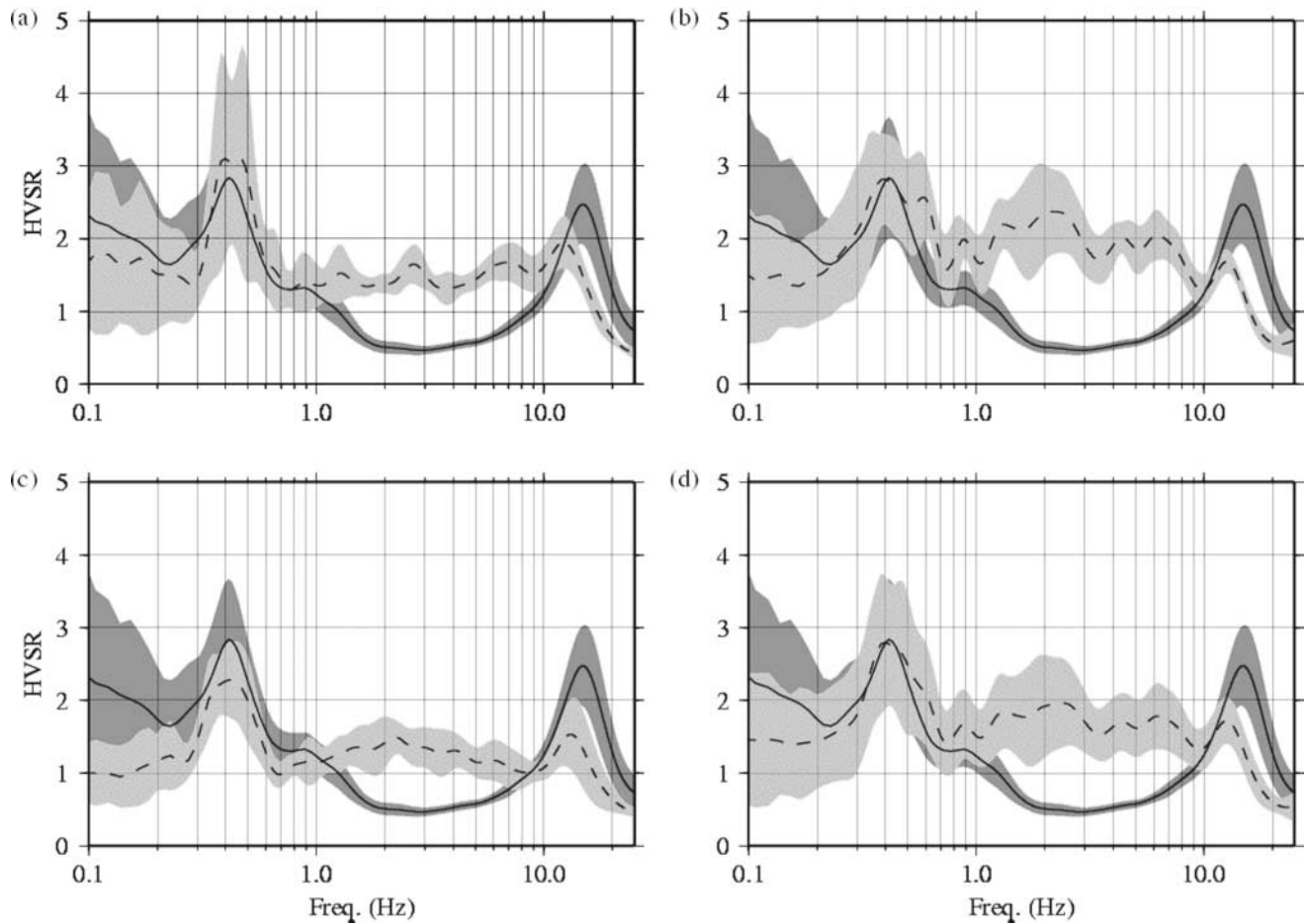


Figure 3. Comparison between the mean spectral ratio of earthquakes (dashed lines) and triggered noise (solid lines). Dark-gray area represents ± 1 S.D. of the triggered noise. Light-gray area represents ± 1 S.D. of (a) the local earthquakes; (b) San Giuliano di Puglia 2002 sequence; (c) regional and teleseismic events; (d) all the analyzed earthquakes.

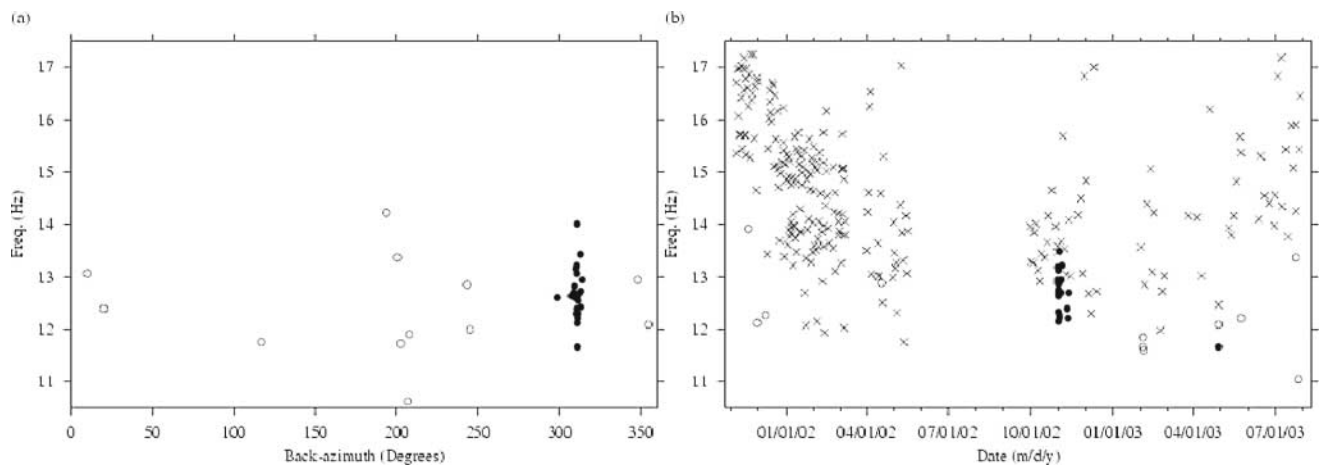


Figure 4. (a) Distribution of the anthropogenic fill fundamental resonance frequency versus the azimuth of the local earthquakes (open circles) and the events of the San Giuliano di Puglia 2002 sequence (filled circles). (b) Temporal distribution of the anthropogenic fill fundamental resonance frequency of the local earthquakes (open circles), the events of the San Giuliano di Puglia 2002 sequence (filled circles), and the triggered noise (\times).

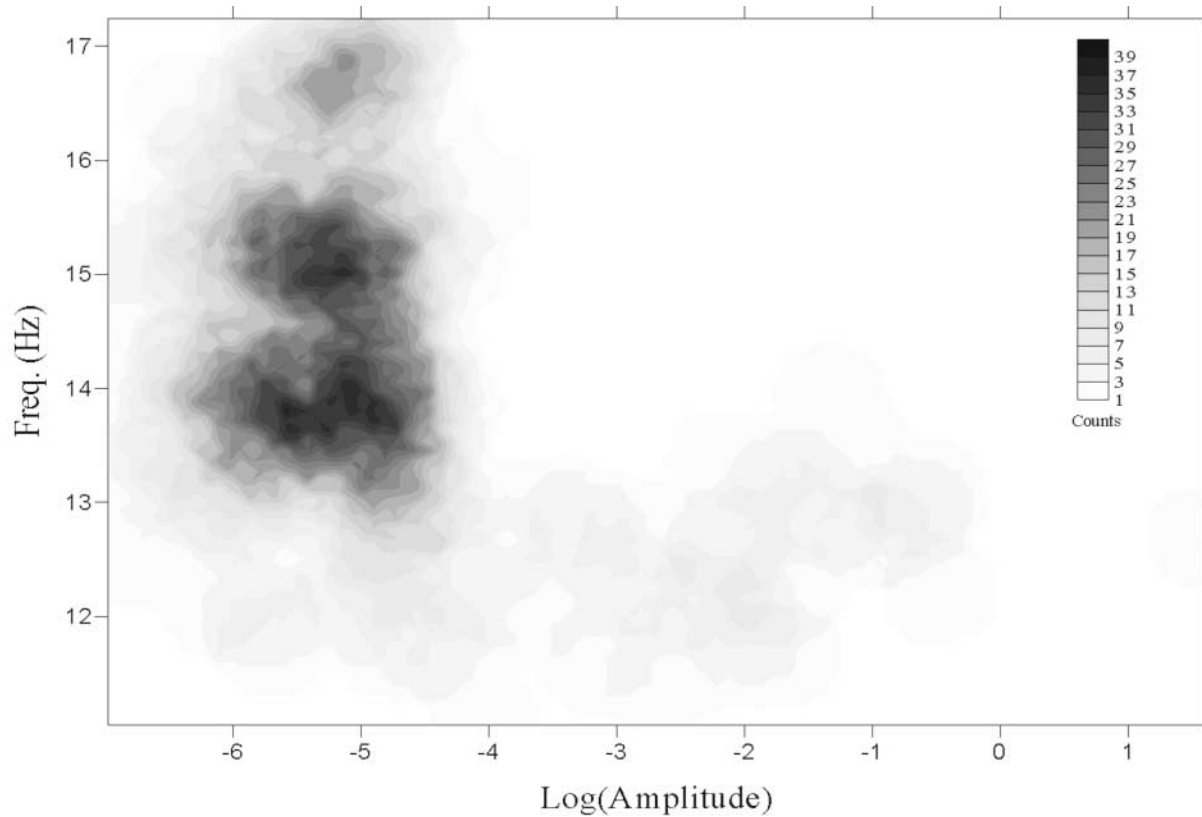


Figure 5. Distribution of the anthropogenic fill fundamental frequency versus the amplitude of all the analyzed signals (triggered noise and earthquakes). See the text for details.

the peak does not occur at frequencies greater than 14 Hz. This behavior hints at the occurrence of nonlinearity, which accounts for the observed misfit of the fundamental resonance frequency of soft soils between weak- and strong-motion records (see Dimitriu *et al.*, 1999; Lacave-Lachet *et al.*, 2000).

By means of the modeling, we try to give an interpretation of the results described in this section. In particular, we concentrate on the absence of the deamplification for the earthquakes and the misfit of the high-frequency peak.

Modeling

Method

We performed the modeling for both the earthquakes and the triggered noise in a layered 1D medium (purely linear), taking advantage of an improved Thomson–Haskell propagator matrix method (Wang, 1999). To compute earthquake synthetic seismograms (noise-free), the algorithm simulates the complete wave field, superimposing three basic Green's functions (strike-slip, dip-slip, and compensated linear vector dipole) for the desired realistic double-couple source mechanism (point source). We used a normalized square half-sinus with a duration of 0.075 sec as source wavelet.

We computed 16 synthetic earthquakes (duration of 56 sec) covering a wide range of epicentral distances and azimuths whose values were taken from local real earthquakes. Because we have no information about their source mechanisms, we set the strike, dip, and rake, respectively, equal to 320°, 40°, and 75°, and the source depth in the range of 8–10 km. In addition we computed synthetic seismograms (whose results are not reported here), varying the source mechanism to verify its influence on the HVSR of synthetic earthquakes, but, except for slight differences at low frequencies, the most important characteristics of the HVSR did not change.

To compute the synthetic noise, we first calculated the Green's functions for a single horizontal force and a single vertical force, both set at the surface and whose source wavelet was the same as that of the synthetic earthquakes. These seismograms were then combined in the following way. For a defined acquisition geometry (array), the original source positions were varied randomly in a predefined region (circular in the range of distances, 1–4 km), and to each varied source a different magnitude was defined (in a predefined range). The time series of the whole array for each varied source was then randomly time lagged to mimic independent firing of the sources, and, finally, the time signals were summed to obtain a noise record at each surface receiver. In

this work, we computed 40 synthetic noise traces whose duration was 52 sec. This duration was chosen to match the window length of the triggered noise.

Models and Comparison with Real Data

Figure 6 shows the comparison of the HVSRs of the real data with the HVSRs of the synthetic ones. The HVSRs of the synthetic seismograms were calculated in the same way as the real ones. Because we have no direct information about the parameters of the layers of the sedimentary cover of the Venosa station site, we first calculated the seismic wave velocities by means of the formula $f = V_s/4h$. Then, we changed the values of the seismic velocities until the synthetic data fit the real data. Tables 4 and 5 show, respectively, the parameters of the 1D layered medium adopted to compute the synthetic earthquakes and the synthetic noise. The parameters of the anthropogenic fill, the conglomerates,

and the clays are reported in bold type. Beneath the clays, we applied the standard crustal model for southern Italy, with the values provided by the National Institute for Geophysics and Volcanology (INGV). The half-space of the model used to simulate the triggered noise (Table 5) is set at 1.319 km (that is the depth of the first layer of the crustal model under the sedimentary cover of the Venosa station site) because the underlying layers of the crustal model have no influence on these simulations. The parameters of the velocity models shown in Tables 3 and 4 are identical except for the seismic wave velocities of the anthropogenic fill. Indeed, to obtain a good fit with the HVSR of triggered noise the S -wave velocity of the anthropogenic fill was set at 215 m/sec, whereas for the HVSR of earthquakes a good fit was obtained with 190 m/sec (Fig. 6a,b). The two values are both in the range of literature values for these kinds of soils (El-gamal *et al.*, 2004). Furthermore, in Figure 6b we note that the HVSR of the synthetic noise computed with $V_s = 190$

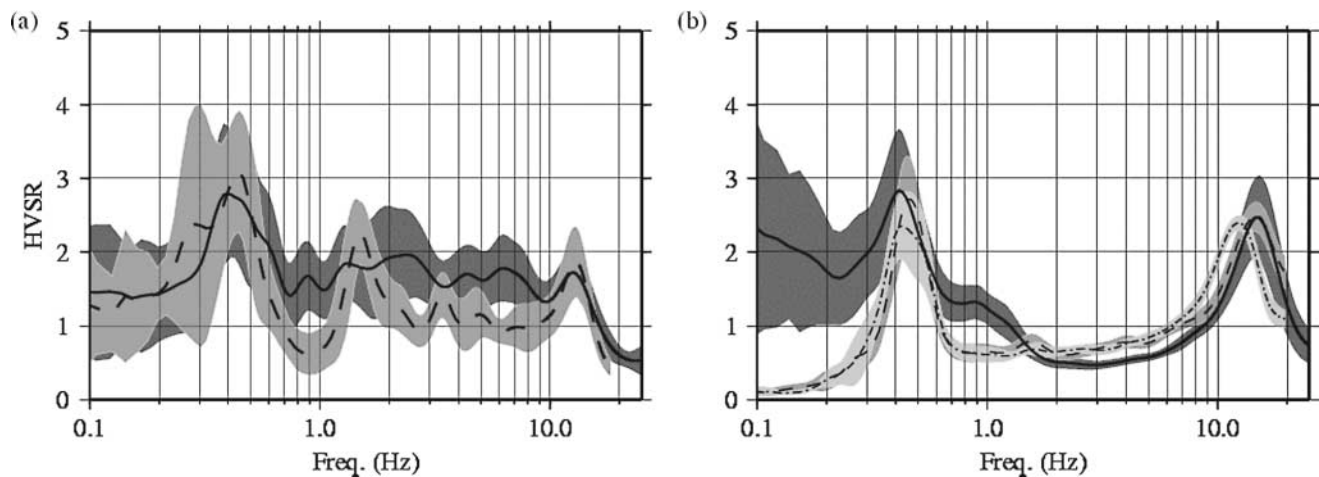


Figure 6. (a) Comparison between the mean spectral ratio of real earthquakes (solid line) and synthetic ones (dashed line). Dark-gray area represents ± 1 S.D. of the real earthquakes. Light-gray area represent ± 1 S.D. of the synthetic earthquakes. (b) Comparison between the mean spectral ratio of triggered noise (solid line), synthetic noise computed with $V_s = 215$ m/sec for the anthropogenic fill (dashed line) and synthetic noise computed with $V_s = 190$ m/sec for the anthropogenic fill (dashed-dotted line). Dark-gray area represents ± 1 S.D. of the triggered noise. Light-gray areas represent ± 1 S.D. of the two HVSRs of the synthetic noise.

Table 4

Parameters of the Velocity Model Used to Compute the Synthetic Earthquakes

| Depth (km) | V_p (km/sec) | V_s (km/sec) | ρ (kg/m ³) | O_p | O_s |
|--------------------|----------------|----------------|-----------------------------|------------|-----------|
| 0–0.004 | 0.329 | 0.190 | 1.5 | 90 | 40 |
| 0.004–0.019 | 1.472 | 0.850 | 2.0 | 168 | 75 |
| 0.019–0.319 | 0.953 | 0.550 | 1.7 | 112 | 50 |
| 0.319–1.319 | 3.0 | 1.732 | 2.2 | 337 | 150 |
| 1.319–3.32 | 3.5 | 2.02 | 2.4 | 450 | 200 |
| 3.32–8.32 | 4.5 | 2.6 | 2.6 | 562 | 250 |
| 8.32–16.32 | 5.2 | 3.0 | 2.8 | 675 | 300 |
| 16.32–30.32 | 6.0 | 3.46 | 3.0 | 787 | 350 |
| ∞ | 8.2 | 4.73 | 3.5 | 1012 | 450 |

Table 5

Parameters of the Velocity Model Used to Compute the Synthetic Noise

| Depth (km) | V_p (km/sec) | V_s (km/sec) | ρ (kg/m ³) | O_p | O_s |
|--------------------|----------------|----------------|-----------------------------|------------|-----------|
| 0–0.004 | 0.372 | 0.215 | 1.5 | 90 | 40 |
| 0.004–0.019 | 1.472 | 0.850 | 2.0 | 168 | 75 |
| 0.019–0.319 | 0.953 | 0.550 | 1.7 | 112 | 50 |
| 0.319–1.319 | 3.0 | 1.732 | 2.2 | 337 | 150 |
| ∞ | 3.5 | 2.02 | 2.4 | 450 | 200 |

m/sec for the anthropogenic fill does not fit the real data. Such a difference of the S -wave velocity corresponds to a degradation of the shear modulus of about 70% (Dimitriu *et al.*, 1999). The degradation might be explained by nonlinear behavior of the anthropogenic fill, as shown by Elgamal *et al.* (2004) and references therein.

Regarding the HVSR of the earthquakes (Fig. 6a), we note that, in general, the site response is well retrieved. In particular, the two peaks of this site are satisfactorily reproduced, the first at low frequency (0.4–0.5 Hz) and the second one at high frequency (about 12.5 Hz). The differences in the frequency range, 1–10 Hz, might be due to the adopted layered 1D model; it is too simple to reproduce the complexities of the crust and of the sedimentary covering as well. Figure 6 shows that in the frequency range 1–8 Hz the HVSR of the earthquakes is not deamplified like the noise HVSR. This effect might be caused by the difference in composition and propagation of the seismic wave field.

Figure 6b highlights the good fit of the HVSR obtained from synthetic noise to the HVSR of the triggered noise. The former reproduces the frequency of the two peaks and also shows the deamplification described previously. The bad fit below 0.3 Hz results from the inadequacy of the procedure to model low-frequency seismic waves.

Conclusions

We investigated the stability of the site response obtained by the HVSR technique at the Venosa station site by analyzing nearly 2 years of data, which are composed of 244 triggered noise recordings and 44 earthquakes, including local, regional, and teleseismic events. The results showed the presence of two distinct peaks: one at low frequency (due to the response of the sedimentary cover overlying the seismic bedrock) and one at high frequency (due to the anthropogenic fill–conglomerates interface).

The results also showed significant differences between the HVSR curves obtained by triggered noise and earthquake recordings. The main difference is the clear deamplification of the triggered noise HVSRs between 1 and 8 Hz compared with the earthquake HVSRs. Using numerical simulations we reproduced these differences and showed that they might be caused by the velocity inversion, which determines the incidence of the seismic waves at the site, and the source position. In fact, because the sources of seismic noise are located at the surface (i.e., above the velocity inversion), the propagation is mainly lateral and the wave field is dominated by surface waves. In contrast, seismic waves from earthquakes propagate nearly vertically through the layers underneath the site because these sources are located at 8–10 km depth. In conclusion, we propose that the difference between the triggered noise and earthquake HVSRs at the Venosa station site stems from the different composition and propagation of the seismic waves.

According to this observation, the presence of the velocity inversion is of essential importance for the site-

response characteristics of the Venosa station site. This result is in contrast to Mucciarelli *et al.* (2003), who showed the high stability of the site response obtained by triggered noise and earthquake data at the Tito Scalo station (southern Italy), a site characterized by monotonically increasing S -wave velocity.

There are practical implications for the results shown here. Seismic noise is widely used in microzonation studies to predict the amplification function of earthquakes, but in the presence of a velocity inversion, as illustrated for the Venosa station site, the deamplification shown by the triggered-noise HVSRs could lead to an underestimation of the amplification function of earthquakes. At least two peaks are present both in the HVSR of the triggered noise and in the HVSR of the earthquakes. It is worth noting that a more simplified amplification study like V_s30 would fail to predict the observed site-response behavior.

The misfit of the peak at high frequency between triggered-noise and earthquake HVSRs correlates neither to azimuthal and/or directional effects, nor to periodicity patterns. Modeling the HVSR of the triggered noise and earthquakes required different S -wave velocities for the anthropogenic fill. This hints at a nonlinear behavior of the anthropogenic fill.

Finally, we conclude with a consideration about the modeling. This task was accomplished by assigning to each layer a constant value of V_p , V_s , ρ , Q_p , and Q_s ; such an exemplification may be valid for the anthropogenic fill and the conglomerates, but probably not for the clays. Indeed, within a thickness of 300 m, it is reasonable to hypothesize the presence of heterogeneities that could lead to variations in the properties of this layer. Thus, a more complex model, especially with regard to the clays, could lead to results that are more able to describe the complexity shown by the HVSR of the real earthquakes.

Acknowledgments

This research was carried out, in part, thanks to an EU ERASMUS mobility grant. We thank Yutaka Nakamura and an anonymous reviewer for their helpful comments.

References

- Bard, P.-Y. (1998). Microtremor measurement: a tool for site effect estimations?, *Proc. of the 2nd International Symposium on the Effects of the Surface Geology on Seismic Motion*, ESG98, Yokohama, Japan, 1251–1279.
- Bonilla, L. F., J. H. Steidl, G. T. Lindley, A. G. Tumarkin, and R. J. Archuleta (1997). Site amplification in the San Fernando Valley, California: Variability of site effect estimation using S -wave, coda, and H/V methods, *Bull. Seism. Soc. Am.* **87**, 710–730.
- Borcherdt, R. D. (1970). Effects of local geology on ground motion near San Francisco Bay, *Bull. Seism. Soc. Am.* **60**, 29–61.
- Castro, R. R., M. Mucciarelli, F. Pacor, and C. Petruccaro (1997). S -wave site response estimates using horizontal-to-vertical spectral ratios, *Bull. Seism. Soc. Am.* **87**, 256–260.
- Dimitriu, P., I. Kalogeras, and N. Theodulidis (1999). Evidence of nonlinear

- site response in horizontal-to-vertical spectral ratio from near-field earthquakes, *Soil Dyn. Earthquake Eng.* **18**, 423–435.
- Elgamal, A., T. Lai, R. Gunturi, and M. Zeghal (2004). System identification of landfill seismic response, *J. Earthquake Eng.* **8**, 545–566.
- Field, E. H., and K. H. Jacob (1995). A comparison and test of various site-response estimation techniques, including three that are non reference-site dependent, *Bull. Seism. Soc. Am.* **85**, 1127–1143.
- Konno, K., and T. Ohmachi (1998). Ground-motion characteristics estimated from spectral ratio between horizontal and vertical components of microtremors, *Bull. Seism. Soc. Am.* **88**, 228–241.
- Lacave-Lachet, C., P.-Y. Bard, J. C. Gariel, and K. Irikura (2000). Straight-forward methods to detect non-linear response of the soil. Application to the recordings of the Kobe earthquake (Japan, 1995), *J. Seism. 4*, 161–173.
- Lachet, C., and P.-Y. Bard (1994). Numerical and theoretical investigations on the possibilities and limitations of the Nakamura's technique, *J. Phys. Earth* **42**, 377–397.
- Lermo, J., and F. J. Chavez-Garcia (1993). Site effect evaluation using spectral ratios with only one station, *Bull. Seism. Soc. Am.* **83**, 1574–1594.
- Mucciarelli, M. (1998). Reliability and applicability of Nakamura's technique using microtremors on the ground surface: an experimental approach, *J. Earthquake Eng.* **2**, 625–638.
- Mucciarelli, M., and M. R. Gallipoli (2001). A critical review of 10 years of microtremor HVSR technique, *Boll. Geof. Teor. Appl.* **42**, 255–266.
- Mucciarelli, M., M. R. Gallipoli, and M. Arcieri (2003). The stability of the horizontal-to-vertical spectral ratio of triggered noise and earthquake recordings, *Bull. Seism. Soc. Am.* **93**, 1407–1412.
- Nakamura, Y. (1989). A method for dynamic characteristics estimations of subsurface using microtremors on the ground surface, *Q. Rept. RTRI Jpn.* **30**, 25–33.
- Nakamura, Y. (2000). Clear identification of fundamental of Nakamura's technique and its applications, no. 2656, *Proc. of the 12th World Conference on Earthquake Engineering*, Auckland, New Zealand.
- Parolai, S., D. Bindi, and P. Augliera (2000). Application of the generalized inversion technique (GIT) to a microzonation study: numerical simulations and comparison with different site-estimation techniques, *Bull. Seism. Soc. Am.* **90**, no. 2, 286–297.
- Parolai, S., P. Bormann, and C. Milkereit (2001). Assessment of the natural frequency of the sedimentary cover in the Cologne area (Germany) using noise measurements, *J. Earthquake Eng.* **5**, 541–564.
- Parolai, S., and S. M. Richwalski (2004). The importance of converted waves in comparing H/V and RSM site response estimates, *Bull. Seism. Soc. Am.* **94**, no. 1, 304–313.
- Parolai, S., S. M. Richwalski, C. Milkereit, and P. Bormann (2004). Assessment of the stability of H/V spectral ratios from ambient noise and comparison with earthquake data in the Cologne area (Germany), *Tectonophysics* **390**, 57–73.
- Riepl, J., P.-Y. Bard, D. Hatzfeld, C. Papaioannou, and S. Nechtschein (1998). Detailed evaluation of site response estimation methods across and along the sedimentary valley of Volvi (EURO-SEISTEST), *Bull. Seism. Soc. Am.* **88**, no. 2, 488–502.
- Wang, R. (1999). A simple orthonormalization method for stable and efficient computation of Green's functions, *Bull. Seism. Soc. Am.* **89**, 733–741.
- Wessel, P., and W. H. F. Smith (1991). Free software helps map and display data, *EOS Trans. AGU* **72**, no. 41, 441, 445–446.
- Department of Structures, Soil Dynamics and Engineering Geology
University of Basilicata
85100 Potenza, Italy
(D.D.G., M.R.G., M.M.)
- GeoForschungsZentrum
14407 Potsdam, Germany
(S.P., S.R.)
- Institute for Environmental Analysis
85050 Tito Scalco (PZ), Italy
(M.R.G.)

Manuscript received 15 December 2004.